

Coesite exsolution from supersilicic titanite in UHP marble from the Kokchetav Massif, northern Kazakhstan

YOSHIHIDE OGASAWARA,^{1,*} KYOKA FUKASAWA,¹ AND SHIGENORI MARUYAMA²

¹Department of Earth Sciences, Waseda University, Nishiwaseda, Shinjuku-ku, Tokyo 169-8050, Japan

²Department of Earth and Planetary Sciences, Tokyo Institute of Technology, Ookayama Meguro-ku, Tokyo 152-8551, Japan

ABSTRACT

Coesite exsolved from supersilicic titanite was discovered in an impure calcite marble at Kumdy-kol in the Kokchetav UHP (ultrahigh-pressure) metamorphic terrane, northern Kazakhstan. This impure marble consists mainly of calcite, K-feldspar, diopside, and symplectites of diopside + zoisite, with minor amount of titanite, phengite, and garnet. No diamond was found in the marble. Coesite and quartz, which have needle or platy shapes measuring about 20–60 μm in length, occur as major exsolved phases in the cores and mantles of titanite crystals with minor calcite and apatite. The strongest Raman band for the coesite needles and plates was confirmed at about 524 cm^{-1} with a weak band at about 271 cm^{-1} . To estimate the initial composition of the titanite before coesite exsolution, exsolved phases were reintegrated by measuring their area fractions on digital images. The highest excess Si in titanite was thus determined to be 0.145 atoms per formula unit (apfu). This composition requires a pressure higher than 6 GPa on the basis of phase relations in the system $\text{CaTiSiO}_5\text{--CaSi}_2\text{O}_5$. This pressure is consistent with other evidence of high pressure in the same marble, such as 1.4–1.8 wt% K_2O and over 1000 ppm H_2O in diopside. Supersilicic titanite and coesite exsolution also indicate that SiO_2 exsolution occurred in the coesite stability field during exhumation of the UHP metamorphic unit.

INTRODUCTION

The Kokchetav terrane (Fig. 1) is well known for its ultrahigh-pressure (UHP) assemblages, such as the first reported occurrence of microdiamond of metamorphic origin (Sobolev and Shatsky 1990). Further studies on metamorphic microdiamond and additional evidence indicative of ultrahigh-pressure metamorphism related to deep continental subduction have been reported from this area: coesite, K-rich clinopyroxene, SiO_2 rods in omphacite, and aluminous titanite (e.g., Sobolev and Shatsky 1990; Zhang et al. 1997; De Corte et al. 1998, 2000; Nakajima et al. 1998; Okamoto et al. 1998, 2000; Ishida et al. 1999; Katayama et al. 2000). In particular, the UHP rocks at Kumdy-kol show the highest-pressure conditions in the Kokchetav terrane and are attracting much attention as examples of the deepest subducted continental material that has been exhumed to the surface. Peak metamorphic conditions of eclogite from the Kumdy-kol have been estimated at >6 GPa and >1000 $^\circ\text{C}$ on the basis of K_2O -in-augite geobarometry and garnet-clinopyroxene geothermometry (Okamoto et al. 1998, 2000). This paper presents the first description of coesite exsolution from titanite and its implications for peak metamorphic P - T conditions of the Kokchetav UHP terrane.

METHODS

Electron microprobe analyses were performed by wavelength dispersive methods (WDS) using a JEOL JXA-8900 Super Probe at Department of Earth Sciences, Waseda Univer-

sity. A LaB_6 filament was used for all analyses. The conditions for spot analyses were an accelerating voltage of 15 kV, a beam current of 20 nA, a beam spot diameter of 2 μm , and a counting interval of 10 s. The data were corrected by the ϕ - ρ - Z method (JEOL 1993). The conditions for X-ray mapping were accelerating voltage of 25 kV, a beam current of 20 nA, a beam spot diameter of 2 μm , and a counting interval for each pixel of 310 ms.

Coesite and other fine-grained minerals were identified with a JASCO NRS-2000 laser Raman spectrometer at the Tokyo Institute of Technology using the 514.5 μm line of an Ar-ion laser at 20 mW and a spot size of 1.0 μm .

Bulk-chemical compositions of titanite with coesite needles and plates were estimated by measuring areal fractions of needles and plates in host grains for a square of $200 \times 200 \mu\text{m}^2$ on the polished surface. Using digital image files of the photomicrographs taken under a reflected-light microscope and laser Raman spectra, needles and plates on the polished surface were discriminated on a computer screen and their areal fractions were calculated by a computer program in *Adobe Photoshop 5.5*.

The discrimination between calcite and dolomite was performed by the staining method using alizarine red S solution. Several grains of calcite were identified by X-ray powder diffraction.

OCCURRENCE

Abundant gneisses and eclogites occur in the Kumdy-kol area, Kokchetav Massif in northern Kazakhstan, and those rocks contain evidence for UHP conditions (e.g., Sobolev and Shatsky 1990; Kaneko et al. 2000; Katayama et al. 2000; Okamoto et

* E-mail: ogasawara@earth.edu.waseda.ac.jp

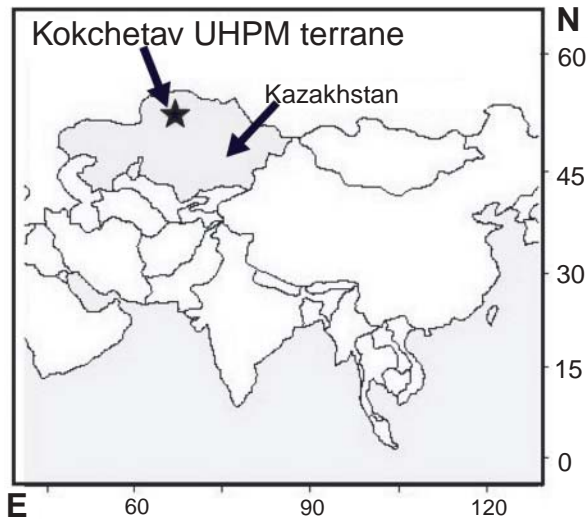


FIGURE 1. Location map of the Kokchetav ultrahigh-pressure metamorphic terrane, northern Kazakhstan.

al. 2000). Impure carbonate rocks also occur as a minor constituent at the Kumdy-kol area.

The metamorphic rocks in this area belong to Unit II of the geologic map by Kaneko et al. (2000). Two types of dolomitic marbles occur in this area; one is diamond-bearing and the other is diamond-free (Ogasawara et al. 2000). These two marbles attained the same metamorphic conditions, and the difference in mineral assemblages of both marbles and the stability relations of diamond can be explained by the local heterogeneity of the fluid compositions, particularly X_{CO_2} , during UHP metamorphism (Ogasawara et al. 2000).

Here we describe a new carbonate rock type from the Kumdy-kol area, a diopside- and K-feldspar-bearing calcite marble that contains titanite with coesite needles and plates. Diopside- and K-feldspar-bearing, calcite marble were collected at a dump site near Kumdy-kol Lake in the Kokchetav Massif. This impure calcite marble lacks microdiamond, however, demonstrating unique UHP mineral chemistry.

Two samples of the marble were analyzed (nos. J76 and J81), and consist mainly of calcite (40%), K-feldspar (30%), diopside (20%), and a symplectite of diopside and zoisite after garnet (<10%), together with a small amount of garnet, titanite, phengite, pyrrhotite, and chlorite. The contents (vol%) of major constituent minerals were roughly estimated under a microscope. This rock exhibits a typical granoblastic texture (Fig. 2A). Coesite needles and plates occur in large grains of titanite in the matrix (Fig. 2B and Fig. 3A) and in an inclusion of titanite (about 0.3 mm in diameter) found within phengite-bearing diopside (Fig. 3B).

Calcite, which is a main constituent of the matrix and also occurs as inclusions in diopside, is almost pure CaCO_3 (MgCO_3 < 1.5 mol%, FeCO_3 < 1.3 mol%, MnCO_3 < 0.8 mol%). K-feldspar occurs in the matrix (0.3–0.5 mm in diameter) and as laths or prisms in diopside. Diopside (from 0.3 to 1.0 mm in diameter) in this marble contains phengite and K-feldspar (lath- or prism-shaped, ca. 100 μm in length) (Fig. 4), which were con-

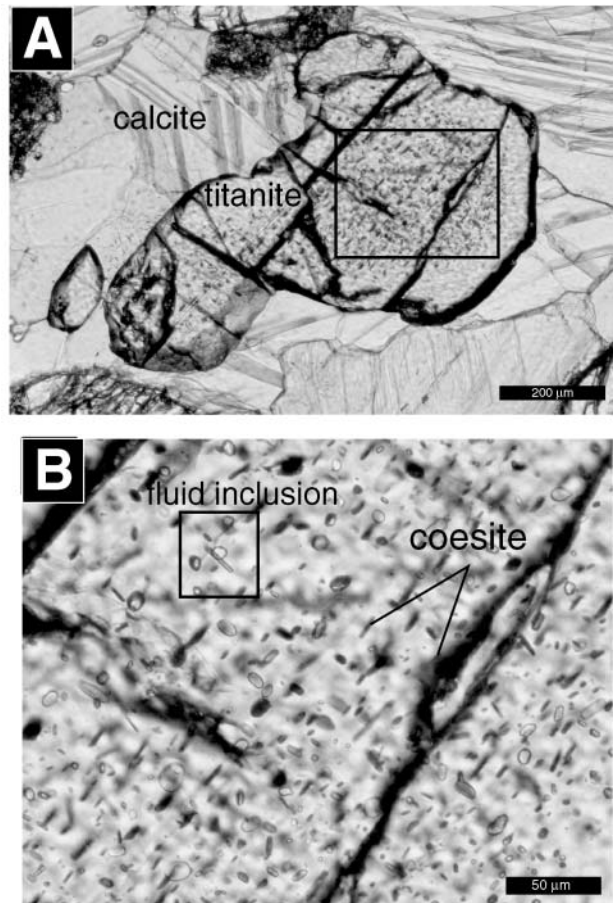


FIGURE 2. Coesite-bearing titanite in calcite marble. (A) Coarser-grained matrix titanite. Scale bar is 200 μm (plane-polarized light). Framed area is shown in B. (B) Coesite needles and plates in titanite shown in A. Scale bar is 50 μm .

firmed by laser Raman spectrometry and by electron microprobe analysis. The host diopside surrounding the K-feldspar lacks phengite needles. The K_2O content of diopside is 0.2–0.7 wt% (Al_2O_3 = 0.9–2.0 wt% and FeO = 1.6–2.1 wt%). Only one garnet grain (about 0.4 mm in diameter) was found as an inclusion in the same grain of phengite-bearing diopside shown in Fig. 3B. The composition of this garnet is (in mol%) $\text{Pyr}_{12.3-14.6}$, $\text{GrS}_{69.9-74.2}$, and $\text{Alm}_{4.8-9.3}$.

The peak metamorphic mineral assemblage was aragonite–diopside–K-feldspar–garnet–phengite–titanite.

TITANITE WITH COESITE EXSOLUTION

Titanite occurs in the matrix and as an inclusion in diopside. Anhedral matrix titanite that forms relatively coarse-grained crystals (0.5 to 2.0 mm in the longest dimension) and contains coesite needles and plates. Finer-grained titanite in the matrix is subhedral to euhedral and does not contain any needles and plates. We found seven grains of matrix titanite with coesite needles and plates. One of these titanite grains contains over a hundred needles and plates, which consist mainly of coesite. Rims of titanite grains lack needles and plates in a zone for several tens of micrometers wide (Fig. 2A).

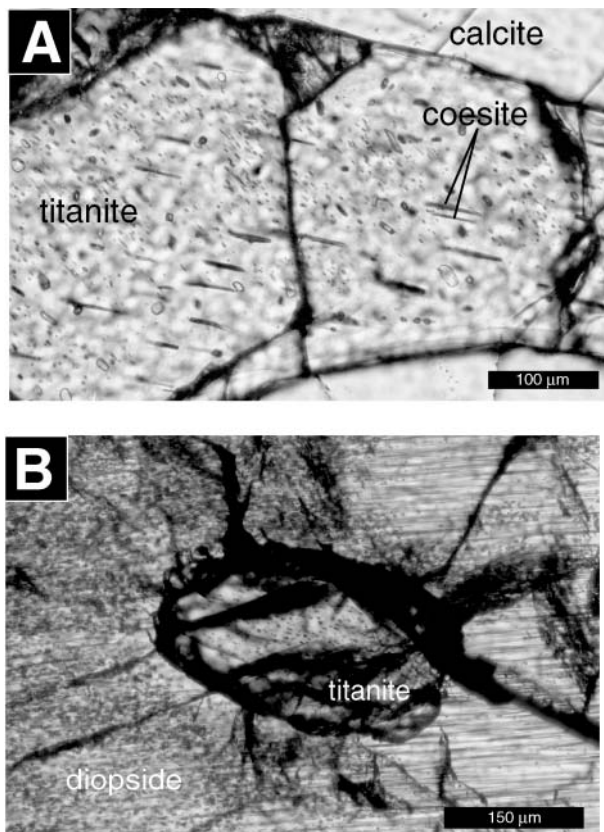


FIGURE 3. (A) Coesite needles in large-grained titanite in matrix (plane-polarized light). Scale bar is 100 μm . (B) Titanite inclusion in diopside with fine rods indicative of coesite and/or quartz. Diopside contains phengite needles. Scale bar is 150 μm .

Two kinds of forms were recognized: needle shaped and platy shaped (Figs. 2B, 3A, and 3B). The needle form was confirmed by observing the shape of cross sections on the polished surface under reflected light. The platy shape was confirmed by changing the focus of the laser in the Raman spectrometer and by observation under an optical microscope. The needles measure 20–60 μm in length and 1–5 μm in width (Figs. 2B and 3A), and the plates 10–20 μm in length (Fig. 2B).

Many of the needles show preferred orientations. As shown in Figure 3A, two orientations were recognized with the dominant direction indicated by longer needles and the other directions by the shorter ones. Platy-shaped coesite does not show a clear preferred orientation.

Two titanite inclusions were found in the same phengite-bearing diopside: one contains coesite needles (Fig. 3B), and the other contains neither needles nor plates. The coesite needles in this titanite inclusion in diopside are shorter than those in matrix titanite: 1 μm in diameter and a maximum 10 μm in length, and they show a preferred orientation in one direction (Fig. 3B). The rims of this titanite inclusion lack coesite needles.

We found a fluid inclusion in matrix titanite with coesite needles and plates (in small frame of Fig. 2B). This fluid inclusion has a rounded platy shape (8 μm in the longer dimension)

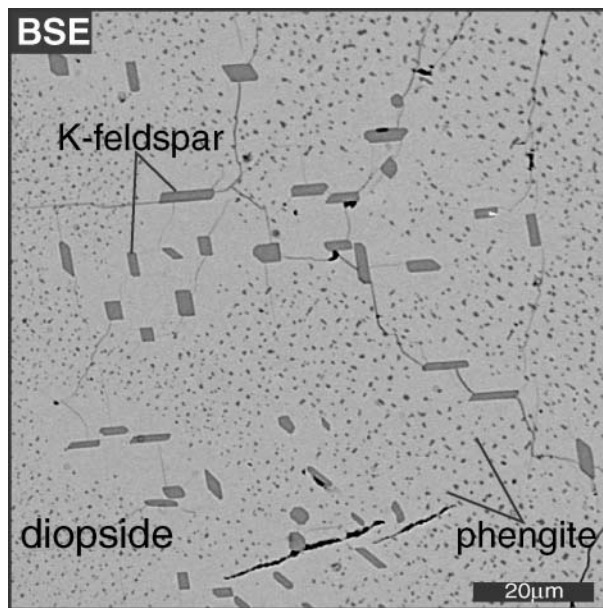


FIGURE 4. Phengite- and K-feldspar-bearing diopside (backscattered electron image). Scale bar is 20 μm .

and consists of liquid and vapor at room temperature. No daughter phase was observed.

By laser Raman spectrometry, we checked almost all of the needle- and platy-shaped phases in titanite that are exposed at the thin section surface. The following minerals and mineral associations (together with titanite) were confirmed to occur: coesite, quartz, coesite + quartz, apatite, calcite, apatite + coesite, apatite + quartz, and calcite + quartz. Among all of the analyzed needles/plates, about 50% were found to be single-phase coesite, about 30% were single-phase quartz, about 10% were coesite + quartz composite grains, about 5% were single phase apatite, and about 5% were single phase calcite. The following associations were confirmed only rarely: apatite + coesite, apatite + quartz, and calcite + quartz. No difference between single-phase and multiphase needles and plates was recognized with the optical microscope.

Representative laser Raman spectra of a coesite needle and a coesite + quartz composite needle are shown in Figure 5. Coesite generally shows strong Raman bands at 521–526 cm^{-1} and weak bands at 176, 271, and 355 cm^{-1} (e.g., Boyer et al. 1985). The coesite in this calcite marble shows the strongest Raman band at about 524 cm^{-1} with a weak band at about 271 cm^{-1} (Fig. 5).

Representative electron microprobe analyses of matrix and inclusion titanites with or without coesite needles and plates are listed in Table 1. A backscattered electron image and X-ray maps for $\text{CaK}\alpha$, $\text{TiK}\alpha$, $\text{SiK}\alpha$, $\text{AlK}\alpha$, and $\text{PK}\alpha$ obtained on a coesite-bearing titanite are shown in Figure 6. Almost all of the analytical values Si concentrate in the range from 0.98 to 1.02 apfu on the basis of 3 cations. Excess Si in the octahedral site is very low in the host titanite and is also low in the rims that lack needles and plates. The concentration of TiO_2 is lower than the stoichiometric value (from 28.4 to 37.3 wt%) and is high in the core and mantle and low at the rim. The Al_2O_3 con-

tent ranges from 1.9 to 6.6 wt% with low values in the core and the mantle (from 2.5 to 4.0 wt%) and higher values at the rim (Fig. 6). TiO_2 and Al_2O_3 exhibit a negative correlation (Table 1 and Fig. 6). Fe_2O_3 is low, 0.0 ~ 0.6 wt%, and shows weak zoning with higher values in the core. MgO is lower than 0.4 wt% and is extremely low at the rim compared with the core and mantle. P_2O_5 reaches concentrations of 0.6 wt% and shows

heterogeneity that is unrelated to the zoning of TiO_2 , Al_2O_3 (Fig. 6). The F content ranges from 0.3 to 3.7 wt%. The titanite inclusion in the phengite-bearing diopside contains 1.9–4.5 wt% of Al_2O_3 .

DISCUSSION

Recently, experimental studies of the phase relations in the system $\text{CaTiSiO}_5\text{--CaSi}_2\text{O}_5$ at pressures from 3.5 to 16.0 GPa at $T = 1350^\circ\text{C}$ demonstrate that the solubility of the CaSi_2O_5 component in titanite, $\text{Ca}(\text{Ti}_{1-x}\text{Si}_x)^{\text{VI}}\text{Si}^{\text{IV}}\text{O}_5$, becomes larger at $P > 5.3$ GPa and $T = 1350^\circ\text{C}$, and the complete solid solution is stable at $P > 8$ GPa (Knoche et al. 1998). These relations are caused by the substitution of Si for Ti in the octahedral site. At these P - T conditions, coesite is the stable SiO_2 polymorphs. These experimental results suggest the possibility of the natural occurrence of supersilicic titanite and its retrograded products in UHP metamorphic rocks, particularly those from the Kokchetav UHP terrane that were subjected to $P >$ several GPa (Okamoto et al. 2000).

There is no direct evidence showing that the coesite needles and plates in the titanite were the products of exsolution from a supersilicic titanite precursor. However, the following facts support the exsolution origin: (1) coesite and its composite grains are extremely fine; (2) the inclusions show typical needle and platy shapes; (3) the needles exhibit preferred orientation in two directions (Fig. 3A), or in one direction (Figs. 1B and 2B); and (4) the lack of needles/plates and the near stoichiometric Si content at the rim of titanite grains indicate overgrowth at a later stage. Considering the experimental phase relations (Knoche et al. 1998) together with such morphological and textural characters, we conclude that the needles and

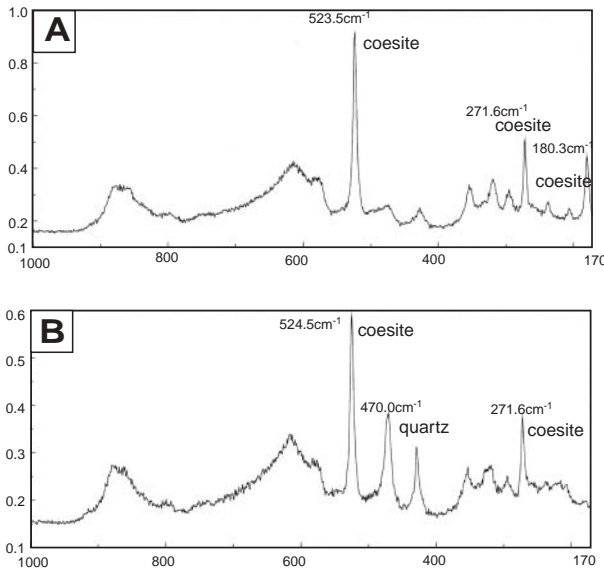


FIGURE 5. Representative laser Raman spectra of exsolved coesite needles in titanite. (A) Raman spectra of coesite. (B) Raman spectra of coesite and quartz composite grain.

TABLE 1. Representative microprobe analyses of titanites

| Sample no. Occurrence | With coesite | | | Without coesite | | |
|------------------------------------------------------------|-------------------|-------------------|-------------------|--------------------|------------------|--------------------|
| | J76b in matrix | J76b in matrix | J76b in matrix | J81 in diopside | J76 in matrix | J81 in diopside |
| SiO_2 | 31.02 | 30.32 | 31.15 | 30.69 | 31.14 | 30.72 |
| TiO_2 | 34.45 | 35.02 | 35.78 | 36.77 | 34.50 | 33.35 |
| Al_2O_3 | 3.67 | 3.16 | 2.93 | 1.94 | 3.24 | 4.30 |
| Cr_2O_3 | 0.03 | 0.00 | 0.06 | 0.00 | 0.08 | 0.00 |
| Fe_2O_3^* | 0.12 | 0.24 | 0.19 | 0.19 | 0.11 | 0.08 |
| MnO | 0.03 | 0.01 | 0.02 | 0.02 | 0.02 | 0.05 |
| MgO | 0.05 | 0.05 | 0.05 | 0.03 | 0.00 | 0.04 |
| CaO | 28.66 | 28.55 | 29.25 | 28.30 | 29.56 | 29.05 |
| Na_2O | 0.02 | 0.00 | 0.00 | 0.05 | 0.00 | 0.00 |
| K_2O | 0.00 | 0.00 | 0.00 | 0.03 | 0.00 | 0.01 |
| P_2O_5 | 0.29 | 0.23 | 0.23 | 0.11 | 0.07 | 0.21 |
| Nb_2O_5 | 0.09 | 0.06 | 0.00 | 0.26 | 0.09 | 0.00 |
| F | 1.37 | 1.89 | 1.30 | 0.73 | 1.60 | 1.96 |
| Total | 99.80 | 99.63 | 100.96 | 99.12 | 100.41 | 99.77 |
| Number of atoms on the basis of three total cations | | | | | | |
| Si | 1.006 | 0.994 | 1.001 | 1.006 | 1.006 | 0.998 |
| Ti | 0.841 | 0.864 | 0.865 | 0.907 | 0.839 | 0.815 |
| Al | 0.140 | 0.122 | 0.111 | 0.075 | 0.123 | 0.165 |
| Cr | 0.001 | 0.000 | 0.002 | 0.000 | 0.002 | 0.000 |
| Fe^{3+} | 0.003 | 0.006 | 0.005 | 0.005 | 0.003 | 0.002 |
| Mn | 0.001 | 0.000 | 0.001 | 0.001 | 0.001 | 0.001 |
| Mg | 0.002 | 0.002 | 0.003 | 0.002 | 0.000 | 0.002 |
| Ca | 0.996 | 1.003 | 1.007 | 0.994 | 1.023 | 1.011 |
| Na | 0.001 | 0.000 | 0.000 | 0.003 | 0.000 | 0.000 |
| K | 0.000 | 0.000 | 0.000 | 0.001 | 0.000 | 0.000 |
| P | 0.008 | 0.006 | 0.006 | 0.003 | 0.002 | 0.006 |
| Nb | 0.001 | 0.002 | 0.000 | 0.004 | 0.001 | 0.000 |
| F | 0.141 | 0.196 | 0.132 | 0.075 | 0.163 | 0.201 |

* Total Fe as Fe_2O_3 .

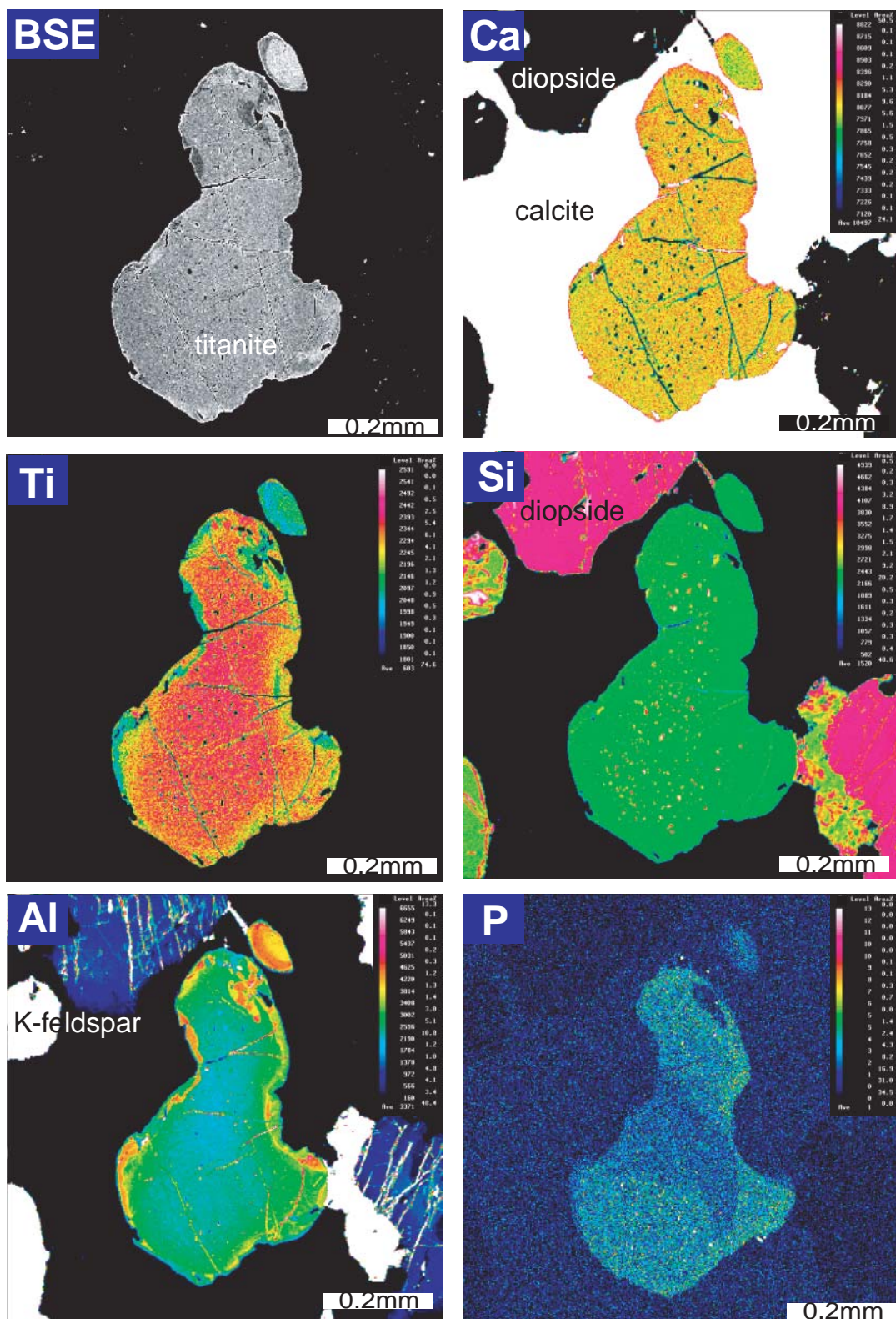


FIGURE 6. Backscattered electron image and characteristic X-ray images for $\text{CaK}\alpha$, $\text{TiK}\alpha$, $\text{SiK}\alpha$, $\text{AlK}\alpha$, and $\text{PK}\alpha$ of coesite-bearing titanite.

plates are the products of exsolution from a supersilicic titanite. We interpret the quartz and calcite found in single and composite needles/plates as the products of retrogression of coesite and aragonite after exsolution.

Coesite exsolution from titanite has two implications with respect to the metamorphic *P-T* conditions of the Kokchetav UHP unit: (1) the peak pressure condition must have been in the stability field of supersilicic titanite and (2) the exsolution of SiO₂ occurred in the stability field of coesite during exhumation. When coesite exsolved from supersilicic titanite, some Ca-bearing phase should have accompanied the coesite, because excess silica corresponds to the CaSi₂O₅ component (Knoche et al. 2000). However, the exsolved phases were mostly coesite and quartz; other phases, apatite and calcite, were detected but are very minor; their volume fractions are unable to satisfy the titanite stoichiometry. Therefore, we cannot specify the exsolution reaction at present.

To approximate the primary composition of titanite before exsolution, the bulk compositions of coesite-bearing titanite were estimated by reintegrating exsolved phases into the host titanite by measuring their fractional areas in a 200 × 200 μm² segment of the thin section. In total, seventeen areas were analyzed. Needles and plates in titanite in analyzed areas consist mostly of coesite and quartz. Calcite was a minor constituent and only the CaO component was reintegrated into the primary titanite when analyzed areas contained calcite. No apatite needle was encountered in some analyzed areas, and its area fractions

were extremely low in others; therefore, the distribution of apatite needles was neglected for this reintegration. Table 2 lists the results for those compositions having relatively high excess Si. The highest SiO₂ content is 34.74 wt%, which corresponds to 1.145 Si apfu. The variation of bulk composition within a single grain reflects the heterogeneous distribution of exsolved phases and may relate to the compositional heterogeneity of primary titanite.

Assuming that the excess Si corresponds to CaSi₂O₅ in titanite, we used the phase relations in the system CaTiSiO₅–CaSi₂O₅ (Knoche et al. 1998) for the pressure estimation. As the temperature dependence of solubility of CaSi₂O₅ in titanite is unclear, we cannot directly use their experimental results at 1350 °C. The peak metamorphic temperature could be located between 980 to 1280 °C on the basis of mineral assemblages found in two associated dolomite-bearing marbles: dolomite-diopside in a diamond-bearing sample and aragonite-forsterite, assuming that *X*_{CO₂} = 0.1 and 0.01 in these dolomitic-bearing marbles, respectively (Ogasawara et al. 2000). Okamoto et al. (2000) reported the peak metamorphic temperature as being greater than 1000 °C. The use of these estimated temperature conditions does not result in large errors when constraining peak metamorphic pressure using the phase relations determined at 1350 °C by Knoche et al. (1998). The highest value of excess Si in titanite (=0.145) corresponds to a pressure at 6 GPa on the solubility curve of the CaSi₂O₅ component (Fig. 7). There is no other constraint for this supersilicic titanite stability; con-

TABLE 2. Bulk compositions of titanites with needles and plates of coesite/quartz and calcite

| | | | | | | | | |
|-------|------------------------------------------------------------|--------|--------|-------|--------|--------|--------|--------|
| area% | titanite | 95.71 | 93.18 | 94.56 | 98.49 | 96.02 | 95.01 | 96.03 |
| | coesite/quartz | 4.29 | 6.82 | 4.11 | 1.51 | 3.98 | 4.99 | 3.97 |
| | calcite | 0.00 | 0.00 | 1.33 | 0.00 | 0.00 | 0.00 | 0.00 |
| wt% | titanite | 96.40 | 94.25 | 95.50 | 98.74 | 96.66 | 95.81 | 96.67 |
| | coesite/quartz | 3.60 | 5.75 | 3.45 | 1.26 | 3.34 | 4.19 | 3.33 |
| | calcite | 0.00 | 0.00 | 1.04 | 0.00 | 0.00 | 0.00 | 0.00 |
| | SiO ₂ | 33.25 | 34.74 | 32.83 | 31.86 | 33.09 | 33.88 | 33.28 |
| | TiO ₂ | 33.98 | 33.23 | 33.67 | 35.11 | 33.87 | 34.07 | 34.38 |
| | Al ₂ O ₃ | 2.82 | 2.76 | 2.80 | 2.63 | 2.90 | 2.55 | 2.58 |
| | Cr ₂ O ₃ | 0.02 | 0.02 | 0.02 | 0.04 | 0.04 | 0.04 | 0.04 |
| | Fe ₂ O ₃ * | 0.10 | 0.10 | 0.10 | 0.27 | 0.27 | 0.26 | 0.26 |
| | MnO | 0.04 | 0.04 | 0.04 | 0.03 | 0.03 | 0.03 | 0.03 |
| | MgO | 0.06 | 0.06 | 0.06 | 0.05 | 0.08 | 0.05 | 0.05 |
| | CaO | 28.06 | 27.44 | 28.38 | 28.45 | 27.95 | 27.61 | 27.86 |
| | Na ₂ O | 0.02 | 0.02 | 0.02 | 0.01 | 0.02 | 0.01 | 0.01 |
| | K ₂ O | 0.01 | 0.01 | 0.01 | 0.04 | 0.01 | 0.04 | 0.04 |
| | P ₂ O ₅ | 0.19 | 0.19 | 0.19 | 0.22 | 0.30 | 0.21 | 0.21 |
| | Nb ₂ O ₅ | 0.06 | 0.06 | 0.06 | 0.07 | 0.08 | 0.06 | 0.07 |
| | F | 1.46 | 1.42 | 1.44 | 1.34 | 1.47 | 1.30 | 1.31 |
| | Total | 100.08 | 100.08 | 99.62 | 100.11 | 100.11 | 100.11 | 100.11 |
| | Number of atoms on the basis of three total cations | | | | | | | |
| | Si | 1.099 | 1.145 | 1.089 | 1.055 | 1.096 | 1.118 | 1.099 |
| | Ti | 0.845 | 0.824 | 0.840 | 0.875 | 0.844 | 0.846 | 0.855 |
| | Al | 0.055 | 0.054 | 0.055 | 0.051 | 0.057 | 0.050 | 0.050 |
| | Cr | 0.000 | 0.000 | 0.000 | 0.000 | 0.001 | 0.000 | 0.000 |
| | Fe ³⁺ | 0.001 | 0.001 | 0.001 | 0.000 | 0.000 | 0.000 | 0.000 |
| | Mn | 0.002 | 0.001 | 0.002 | 0.001 | 0.002 | 0.001 | 0.001 |
| | Mg | 0.001 | 0.001 | 0.001 | 0.000 | 0.001 | 0.000 | 0.000 |
| | Ca | 0.994 | 0.969 | 1.009 | 1.009 | 0.992 | 0.976 | 0.986 |
| | Na | 0.000 | 0.000 | 0.000 | 0.001 | 0.000 | 0.001 | 0.001 |
| | K | 0.003 | 0.003 | 0.003 | 0.003 | 0.004 | 0.003 | 0.003 |
| | P | 0.001 | 0.001 | 0.001 | 0.003 | 0.003 | 0.003 | 0.003 |
| | Nb | 0.000 | 0.000 | 0.000 | 0.000 | 0.000 | 0.000 | 0.000 |
| | F | 0.076 | 0.074 | 0.076 | 0.070 | 0.077 | 0.068 | 0.068 |

* Total Fe as Fe₂O₃.

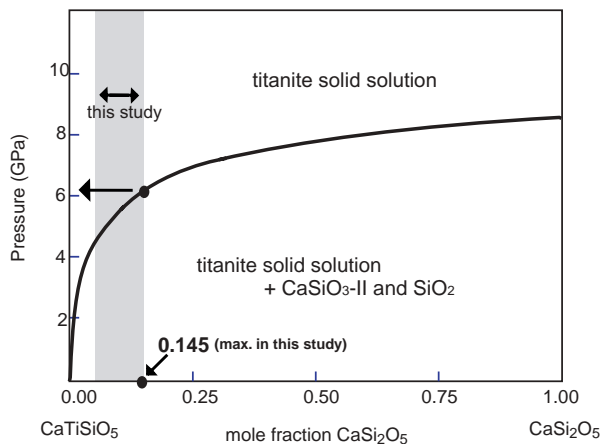


FIGURE 7. *P-X* diagram for the system $\text{CaTiSiO}_5\text{-CaSi}_2\text{O}_5$ at 1350 °C (Knoche et al. 1998) showing the mole fraction of CaSi_2O_5 in titanite before coesite exsolution as obtained in this study (shaded area).

sequently, this value approximates the minimum pressure. The titanite with exsolved coesite in this calcite marble indicates the stability of supersilicic titanite, and implies that the peak metamorphic pressure had been higher than 6 GPa.

Diopside in this marble contains phengite needles and some diopside crystals contain both phengite and K-feldspar (Fig. 4). If these K_2O -bearing phases in diopside are of exsolution origin from K_2O - and H_2O -bearing diopside, the original composition of the diopside requires a very high-pressure condition. The bulk K_2O content of this diopside ranges from 1.4 to 1.8 wt% for the domain showing K-feldspar exsolution (Muko et al. 2001). The K_2O solubility in clinopyroxene is an indicator of UHP conditions (e.g., Schmidt 1996; Harlow 1997; Luth 1997; Okamoto and Maruyama 1998), and high- K_2O clinopyroxene has been reported for diamond-grade eclogites of the Kumdy-kol area (Shatsky et al. 1995; Zhang et al. 1997; Okamoto et al. 1998, 2000).

Locke et al. (2000) reported that clinopyroxene contains 1400 to 1600 ppm H_2O at 7.5 GPa and 1200 °C, whereas H_2O is 80 to 120 ppm at 5 GPa and 1150 °C. Assuming that phengite in the diopside is of exsolution origin, then the bulk H_2O content of the diopside—roughly estimated from the areal fraction of phengite—was about 1000 ppm H_2O for the domain having phengite needles. This reintegration ignores the H_2O contents of host diopside. Preliminary micro-FT-IR results on this diopside suggest that the diopside near the exsolved K-feldspar may contain more than 1000 ppm H_2O (Fukasawa et al. 2001). These findings are also indicative of pressure conditions higher than 5 GPa.

The maximum pressure for the peak of metamorphism can be estimated from the upper pressure stability limit of dolomite, as this mineral was stable in diamond-bearing and in diamond-free dolomitic marbles (Ogasawara et al. 2000). A recent multianvil study showed that the dissociation of dolomite into aragonite + magnesite depends on temperature, and occurs at ~7.5 GPa at 1000 °C and ~8.8 GPa at 1200 °C (Sato and Katsura 2000). Consequently, the peak metamorphic pressure of the Kumdy-kol area must be between 6 and 9 GPa. Coesite

exsolution from supersilicic titanite also suggests that the solubility of CaSi_2O_5 in titanite was very low, with pressure conditions near the lower limit of the coesite stability field.

SUMMARY

Exsolved needles and plates of coesite in titanite, together with other exsolved phases, including quartz after coesite, minor calcite, and apatite, were discovered in impure calcite marble at Kumdy-kol in the Kokchetav UHP metamorphic terrane, northern Kazakhstan. This is the first discovery of coesite of exsolution origin in UHP metamorphic rocks and is also the evidence for the presence of supersilicic titanite in the $\text{Ca}(\text{Ti}_{1-x}\text{Si}_x)^{\text{VI}}\text{Si}^{\text{IV}}\text{O}_5$ structure. This discovery of coesite exsolution from supersilicic titanite thus adds another unique feature to the Kokchetav UHP carbonate rocks. Coesite exsolution suggests that the solubility of CaSi_2O_5 in titanite is very low, even in the coesite stability field, consistent with recent experimental studies (Knoche et al. 1998).

The maximum amount of excess Si in titanite was estimated at 0.145 apfu by the reintegration of exsolved phases. This value gave a minimum peak metamorphic pressure of about 6 GPa (Knoche et al. 1998). Combining the upper pressure limit of dolomite in the two dolomite-bearing marbles with this minimum *P* value, the peak metamorphic condition constrained by the Kokchetav carbonate rocks can be estimated in the range from 6 to 9 GPa. Other evidence of high pressure, such as K_2O - and H_2O -bearing diopside, also supports this estimate of peak metamorphic pressure conditions.

ACKNOWLEDGMENTS

The authors thank B.R. Frost, C. Chopin, and B. Durtrow for their reviews and suggestions for improving this paper. We are grateful to K. Okamoto, S. Omori, and I. Katayama for their helpful advice and discussions. We are also deeply grateful to the Japanese mapping team for their fieldwork and collecting many exciting rock samples. We also thank K. Saga and K. Yonemochi for their assistance with the laboratory work. This study was financially supported in part by the Waseda University Grant for the Special Research Project no. 99A-518, the Grant of RISE of Waseda University Project no. B-240, and the Grant in Aid of the Ministry of Education and Science no. 13640485.

REFERENCES CITED

- Boyer, H., Smith, D.C., Chopin, C., and Lasnier, B. (1985) Raman microprobe (RMP) determinations of natural and synthetic coesite. *Physics and Chemistry of Minerals*, 12, 45–48.
- De Corte, K., Cartigny, Y., Shatsky, V.S., Sobolev, N.V., and Javoy, M. (1998) Evidence of fluid inclusions in metamorphic microdiamonds from the Kokchetav massif, northern Kazakhstan. *Geochimica et Cosmochimica Acta*, 62, 3765–73.
- De Corte, K., Korsakov, A., Taylor, W.R., Cartigny, P., Ader, M., and De Paeppe, P. (2000) Diamond growth during ultrahigh-pressure metamorphism of the Kokchetav Massif, northern Kazakhstan. *The Island Arc*, 9, 428–438.
- Fukasawa, K., Ogasawara, Y., and Maruyama, S. (2001) Coesite exsolution, silica-excess titanite and K_2O -, H_2O -bearing diopside in calcite marble from the Kokchetav UHP terrane. Abstract of Goldschmidt Conference, 2001, no. 3549.
- Harlow, G.E. (1997) K in clinopyroxene at high pressure and temperature: An experimental study. *American Mineralogist*, 82, 259–269.
- Ishida, H., Ogasawara, Y., Ohta, M., and Osumi, K. (1999) Microalae X-ray diffraction study on microdiamonds from Kumdy-kol in the Kokchetav UHP terrane, northern Kazakhstan. *EOS Transactions of the American Geophysical Union*, 80, F986.
- JEOL Ltd. (1993) Program for ϕ - ρ - Z quantitative analysis. Instructions XM-87452/Z2328T, 1–7.
- Kaneko, Y., Maruyama, S., Terabayashi, M., et al. (2000) Geology of the Kokchetav ultrahigh-pressure-high-pressure metamorphic belt, north-eastern Kazakhstan. *The Island Arc*, 9, 264–283.
- Katayama, I., Zayachkovsky, A.A., and Maruyama, S. (2000) Prograde pressure-temperature records from inclusions in zircon from ultrahigh-pressure-high-pressure rocks of the Kokchetav Massif, northern Kazakhstan. *The Island Arc*,

- 9, 417–427.
- Knoche, R., Angel, R., Seifert, F., and Fliervoet, T. (1998) Complete substitution of Si for Ti in titanite $\text{Ca}(\text{Ti}_{1-x}\text{Si}_x)\text{SiO}_6$. *American Mineralogist*, 83, 1168–1175.
- Locke, D.L., Holloway, J.R., and Hervig, R. (2000) Experimental Determination of H_2O Solubility in Mantle Clinopyroxene at 5 and 7.5 GPa. *EOS Transactions of the American Geophysical Union*, 81, S444.
- Luth, R.W. (1997) Experimental study of the system phlogopite-diopside from 3.5 to 17 GPa. *American Mineralogist*, 82, 1198–1209.
- Muko, A., Ogasawara, Y., Fukasawa, K., and Zhu, Y. (2001) K_2O -, H_2O -bearing diopside in UHP calcite marble from the Kokchetav Massif. Abstract of Sixth International Eclogite Conference, 96.
- Nakajima, Y., Okamoto, K., Maruyama, S., Ogasawara, Y., and Liou, J.G. (1998) Ti-clinohumite-bearing garnet peridotite from Kumdy-kol area in the Kokchetav UHP complex, northern Kazakhstan. *EOS Transactions of the American Geophysical Union*, 79, W129.
- Ogasawara, Y., Ohta, M., Fukasawa, K., Katayama, I., and Maruyama, S. (2000) Diamond-bearing and diamond-free metacarbonate rocks from Kumdy-kol in the Kokchetav Massif, northern Kazakhstan. *The Island Arc*, 9, 400–416.
- Ogasawara, Y., Ohta, M., Ishida, H., and Fukasawa, K. (2001) Unique high pressure evidence in the Kokchetav UHP carbonate rocks. Abstract of Goldschmidt Conference 2001, no. 3545.
- Okamoto, K. and Maruyama, S. (1998) Multi-anvil re-equilibration experiments of Dabie Shan ultrahigh-pressure eclogite within the diamond-stability fields. *The Island Arc*, 7, 52–69.
- Okamoto, K., Maruyama, S., Liou, J.G., and Ogasawara, Y. (1998) Petrological study of the diamond-grade eclogite in the Kokchetav massif, northern Kazakhstan. *EOS Transactions of the American Geophysical Union*, 79, F988.
- Okamoto, K., Liou, J.G., and Ogasawara, Y. (2000) Petrology of the diamond-grade eclogite in the Kokchetav Massif, northern Kazakhstan. *The Island Arc*, 9, 379–399.
- Sato, K. and Katsura, T. (2001) Experimental investigation on dolomite dissociation into aragonite + magnesite up to 8.5 GPa. *Earth and Planetary Science Letters*, 184, 529–534.
- Schmidt, M.W. (1996) Experimental constraints on recycling of potassium from subducted oceanic crust. *Science*, 272, 1927–1930.
- Shatsky, V.S., Sobolev, N.V., and Vavilov, M.A. (1995) Diamond-bearing metamorphic rocks of the Kokchetav Massif (northern Kazakhstan). In R.G. Coleman and X. Wang, Eds., *Ultrahigh-pressure metamorphism*, p. 427–455. Cambridge University Press, Cambridge, U.K.
- Sobolev, N.V. and Shatsky, V.S. (1990) Diamond inclusions in garnets from metamorphic rocks. *Nature*, 343, 742–746.
- Zhang, R.Y., Liou, J.G., Ernst, W.G., Coleman, R.G., Sobolev, N.V., and Shatsky, V.S. (1997) Metamorphic evolution of diamond-bearing and associated rocks from the Kokchetav Massif, northern Kazakhstan. *Journal of Metamorphic Geology*, 15, 479–496.

MANUSCRIPT RECEIVED MAY 2, 2001

MANUSCRIPT ACCEPTED DECEMBER 4, 2001

MANUSCRIPT HANDLED BY BARB DUTROW